Molina, S.; Guardiola, C.; Martín Díaz, J.; Garcia Sarmiento, D. (2014). Development of a control-oriented model to optimise fuel consumption and NOX emissions in a DI Diesel engine. Applied Energy. 119:405-416. doi:10.1016/j.apenergy.2014.01.021.

Development of a control-oriented model to optimise fuel consumption and NO_X emissions in a DI Diesel engine.

S. Molina, C. Guardiola, J. Martín*, D. García-Sarmiento

CMT-Motores Térmicos, Universitat Politècnica de València, Camino de Vera s/n, 46022, Valencia, Spain

Abstract

This paper describes a predictive model of NO_X and consumption oriented to control and optimisation applications in DI Diesel engines. The model, which is based on the Response Surface Methodology (RSM), is focused on the prediction of NO_X emissions and brake specific fuel consumption (output parameters) following a two step process: first, the relationship between engine inputs and combustion parameters is determined and, secondly, engine outputs are predicted from the combustion parameters, taking into account the mechanical losses. The inputs are engine variables related to the intake charge conditions (exhaust gas recirculation rate, intake pressure and temperature), injection settings (start of main and pilot injections, and injection pressure), and some combustion parameters that allow to characterise the in-cylinder gas processes (peak pressure, indicated mean effective pressure and burned angles). Splitting the model into two parts allows using either experimental or modelled combustion parameters, thus enhancing the model flexibility. The proposed model is finally used for multi-objective optimisation of engine operation.

Keywords: engine performance, in-cylinder pressure, NO_X emissions, Response Surface Methodology, predictive model

*Corresponding author. Tel: +34963877650; fax: +34963877659
Email address: jaimardi@mot.upv.es (J. Martín)
URL: www.cmt.upv.es (J. Martín)

Nomenclature

amep	auxiliary mean effective pressure	$[bar]$
B%	burned angle (after top dead centre)	$[^\circ ATDC]$
bmep	brake mean effective pressure	$[bar]$
bsfc	brake specific fuel consumption	$[g/kWh]$
DOE	Design Of Experiments	
EGR	Exhaust Gas Recirculation	
F_r	relative fuel/air equivalence ratio	$[-]$
HRL	Heat Release Law	$[J]$
ICE	Internal Combustion Engine	
imep	indicated mean effective pressure	$[bar]$
$\dot{m}$	mass flow	$[g/s]$
m	mass	$[kg/str]$, $[mg/str]$
MPC	Model Predictive Control	
n	engine speed	[rpm]
p	pressure	$[bar]$
pmep	pumping mean effective pressure	$[bar]$
RoHR	Rate of Heat Release	$[J/\circ]$
RSM	Response Surface Methodology	
SOC	Start Of Combustion	$[^\circ ATDC]$
SOI	Start Of Injection	$[^\circ ATDC]$
T	temperature	$[K]$, $[^\circ C]$
fmep	friction mean effective pressure	$[bar]$
V	volume	$[m^3]$

Subindex

cyl	in-cylinder
exh	exhaust manifold
f	fuel
inj	injection
itk	intake manifold
m	mean value
$main$	main injection
max	maximum value
oil	oil
pil	pilot injection

Greek symbols

α	optimisation weight factor
β	gradient of the merit near the optimum value

1. Introduction

In the last two decades regulations and market demands have lead to improve internal combustion engines (ICE) control systems [1, 2], accelerating the evolution of new forms of design. Moreover, next generations of Diesel engines will probably include more sophisticated control systems than those in use today because they will incorporate some combination of VGT, variable rate fuelling, exhaust after-treatment, EGR, cylinder pressure sensors and emission sensors among others [3, 4].

The variables involved in ICE control can be classified into three types: inputs that con be modified (injection and air management settings), variables that provide information of the real system state (speed, pedal position, pressure and temperature of different fluids at different locations, etc) and finally the engine outputs (performance and emissions). The classical approach for calibration and control is based on lookup tables in which the optimal combination of inputs, obtained from measurements in stationary operating points, is tabulated in terms of engine speed and load [5]. This procedure takes into account the relationship between inputs and outputs to achieve the desired engine response based on a recorded feed-forward control action. However, engine calibration systems based on lookup tables are reaching the limits of their applicability, as they require too much time and effort to be tuned [6], and they are not optimal under variations in the engine operating conditions.

In this scenario, modern control techniques offer several tools that allow overcoming the stated problem. One of the most efficient approaches is the use of control-oriented predictive models, suitable for the control of systems characterised by a complicated dynamic, multivariable or unstable behaviour [7, 8, 9, 10]. In some cases, these models can adapt to the engine changes along time, ensuring the same operation from the factory calibration until after several thousand hours of use [11]. This control strategy uses predictive mathematical models of the processes in order to estimate the future behaviour of the system for given control inputs, thus optimising the selection of the control signals [1, 6, 10, 12, 13, 14, 15, 16]. In this scenario, in-cylinder pressure provides direct information on combustion development [6, 17, 18, 19, 20, 21], as peak pressure, indicated mean effective pressure or heat release. Thus, in-cylinder pressure can be used in different engine control applications such as failure detection [21], air mass flow estimation [22], on-line combustion detection [23], exhaust gas recirculation control [12, 24], torque estimation [25], noise control [26] or NO_X control [27].

Several works dealing with the combined use of in-cylinder pressure and predictive models for control purposes can be found in literature, ranging from simple to very complex methods. Reitz et al. [28] use the pressure peak to set the injection settings in split injection strategies. Leonhardt et al. [21] control the fuel injection and spark timing with a feed-forward emission control strategy based on the pressure peak. Zhu et al. [20] use the pressure peak location, the angle of 50% mass fraction burned (B50) and the pressure ratio in order to find the best spark timing for maximum brake torque. Beasley et al. [29] control the angle of B50, limiting the peak pressure in the chamber and establishing combinations of these parameters for engine protection and combustion stability. Win et al. [30] analyse the start of injection, ignition delay, rate of pressure rise,

and rate of heat release, to obtain correlations via the Response Surface Methodology (RSM) to carry out a multi-objective optimisation of combustion noise, brake specific fuel consumption (bsfc), HC, soot and NO_X. Several complex models based on neural networks [31], genetic algorithms or fuzzy-logic [11] use the information of the combustion development (derived from the heat release law) along with several engine mean variables for accurate predictions of emission and performance.

This paper proposes a methodology for obtaining an empirical model capable of predicting both the engine consumption and NO_X emissions of a DI Diesel engine. Unlike the proposals of Reitz et al. [28], Leonhardt et al. [21] or Zhu et al. [20], the model is not focused on the disturbance of one specific parameter but it considers all the relevant ones related to intake charge conditions, injection settings and combustion parameters. The use of RSM allowed maintaining the model simplicity.

As detailed in the Methodology section, one contribution of the work is splitting the model into two parts: the first is focused on the relationship between inputs and in-cylinder conditions while the second deals with in-cylinder condition and outputs. This way of proceeding allowed following and comparing two alternative paths: modelling the key in-cylinder parameters (imep, p_{max} and burned angles) or obtaining them from the experimental pressure, thus enhancing the model flexibility.

Finally, as described in section 7, once the bsfc and NO_X models were developed, a multi-objective optimisation was performed to find the best inputs combination that minimises bsfc and NO_X simultaneously, while respecting some constraints.

2. Experimental setup

A scheme of the test cell layout with the instrumentation is shown in Fig. 1. For the sake of accuracy, the experimental tests were carried out in a single-cylinder 0.4 litre DI Diesel engine whose 4-cylinder engine version is currently in production. The engine main characteristics are given in Table 1. The engine settings of the reference operating point were taken from the Euro 5 ECU map of the 4-cylinder engine version. The engine was directly coupled to an electric dynamometer that allows controlling the engine speed and load.

Bore	76 mm
Stroke	88 mm
Unitary piston displacement	399.2 cm^3
Connecting rod length	123.8 mm
Compression ratio	17:1
Injection	Bosch common rail

Table 1: Engine characteristics.

The installation includes an EGR conditioning system that takes the gas from the exhaust settling chamber, uses a gas-water heat exchanger to cool and dry it, and then a

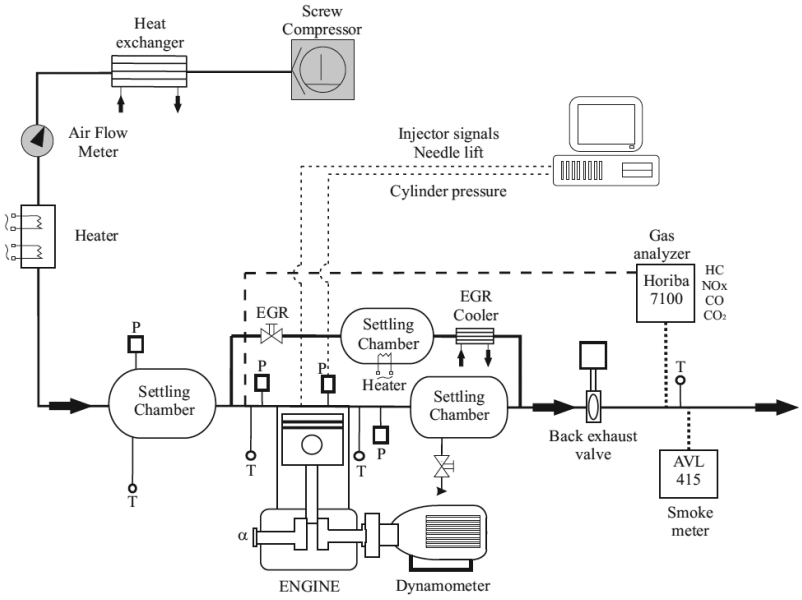

Figure 1: Experimental setup.

heater to reach the desired EGR temperature before mixing it with the fresh air. Also, the fresh air can be conditioned to the required temperature. Thus, the intake temperature (after mixing fresh air and EGR) can be accurately controlled according to the experimental test requirements. The exhaust back pressure produced by the turbine in the 4-cylinder engine version is reproduced by a valve in the exhaust system that controls the pressure in the exhaust settling chamber.

The in-cylinder pressure was measured by means of a Kistler 6055B glow-plug piezoelectric transducer with a range between 0 and 250 bar, and a sensitivity of 18.8 pC/bar. The pressure sensor was calibrated according to the traditional method proposed in [32]. The electrical charge yielded by the piezoelectric transducer is converted into a proportional voltage signal by means of a Kistler 5011B charge amplifier. A crank angle increment of 0.2° was used for the in-cylinder pressure acquisition, which was performed using a Yokogawa DL708E oscillographic recorder with a 16 bits A/D converter module.

Some mean variables, used for controlling the engine operation and also required for model development, were acquired at a low sample frequency of 100 Hz using an AVL test system, that collects the measurement signals of the different sensors and controls the electric dynamometer.

The exhaust emissions were analysed and recorded using a Horiba MEXA 7100 D. The EGR flow rate estimation was carried out using experimental measurements of intake and exhaust CO_2 concentrations.

3. Methodology

Two important issues must be considered regarding the model development. The first is the model scope from the point of view of the number of inputs. The methodology followed, a combination of Design of Experiments (DOE) and Response Surface Methodology (RSM) [30, 33, 34], allowed considering a complete list of inputs related with both the injection and air management settings, and some combustion parameters, while maintaining an affordable experimental work. The statistical analysis allowed to select the most relevant ones for the output prediction. The result is a model that considers all the relevant parameters while maintaining the simplicity.

The second issue is the range of operating points that can be covered. If the complete engine map had been considered, the great amount of information to be managed would have lead to the use of a complex model because it is not possible to replace a complete cartography with some simple expressions while maintaining a good predictive capacity [30]. Thus, this work is focused on the local modelling to predict the effect of all the relevant disturbance around a reference point. As EGR has a big influence on NO_X emissions, a reference point with high EGR rate was used: a mid speed (2000 rpm) and 40% load operating point which nominal settings are given in Table 2. The extension of the proposed model to cover different speeds and loads is out of the scope of this paper, but it can be done via a local correction similar to that proposed in a previous work [27].

	Studied range			
Studied parameter	Nominal	Min	Max	Units
EGR	15	0	30	[%]
Intake Pressure (p_{itk})	1.6	1.4	1.8	[bar]
Intake Temperature (T_{itk})	51	41	61	[°C]
Exhaust Pressure (p_{exh})	1.7	1.5	1.9	[bar]
Injection pressure (p_{inj})	1235	1035	1435	[bar]
Injected fuel mass (m_f)	19.5	-	-	[mg/str]
Start of pilot injection (SOI_{pil})	-34	-38	-30	[°ATDC]
Start of main injection (SOI_{main})	-5	-9	-1	[°ATDC]

Table 2: Operating point parameters.

For the model development, the response of some in-cylinder parameters was identified by varying the inputs around the reference operating point. On one hand, burned angles (B%) are the best way to characterise the combustion development which has a direct influence on emissions [27]. On the other hand, imep, combined with a mechanical losses model, can provide a good estimation of the brake mean effective pressure (bmep) and engine consumption (bsfc). Based on these in-cylinder parameters and some inputs, expressions for bsfc and NO_X emissions (engine outputs) were derived. The following steps were considered:

1. Inputs selection: once the reference operating point was selected, in order to design the parametric study [30, 35, 36], the most influential input variables and

their variations were chosen. For this purpose, a preliminary simple effect study was carried out. Its objective is to assess the influence of different air management variables and injection settings on the heat release law and engine outputs, thus discarding the variables with negligible effect for the complete experimental design. More detailed description of this issue is provided in section 4.

2. Calculation of the in-cylinder parameters response surfaces: the in-house combustion analysis tool CALMEC [27, 37, 38, 39] was used to obtain the in-cylinder parameters from experimental pressure, such as burned angles, imep and p_{max}. Then, the RSM methodology was applied in order to obtain mathematical expressions that correlate these parameters with the input variables. Section 5 is devoted to explaining this issue.

3. Calculation of the output response surfaces: on one hand, starting from the expression of the imep obtained in the previous step and applying a mechanical losses model, the bmep and bsfc were obtained; on the other hand, the NO_X emissions were correlated with the HRL [27] through the burned angles and also some inputs, as explained in section 6.

A second-order model was used for the response surface correlations and thus an orthogonal experimental design was required [28, 30]. A Box-Behnken design centred on the reference operating point and the parameters variation defined during the inputs selection were used. The last two steps dealt with the Analysis of Variance (ANOVA) that allowed identifying the interactions with statistical influence, and the response surface determination.

4. Inputs selection

Firstly, the most influential air management parameters (EGR rate, intake pressure -p_{itk}- and temperature -T_{itk}-) and injection settings (injection pressure -p_{inj}- and start of main or pilot injections -SOI_{main}, SOI_{pil}-) that affect NO_X formation were evaluated in some simple effect tests (one parameter is modified while keeping constant the rest). Their variation ranges are given in the third and fourth columns of Table 2. All the variation ranges are centred on the nominal value (second column). The main in-cylinder parameters and outputs results are shown in Table 3.

The nominal EGR rate is 15%; maintaining the rest of parameters, the maximum EGR rate to avoid soot emission higher to 2 FSN is about 30%, hence its variation range was set from 0% up to 30%. Table 3 and Fig. 2 show that increasing EGR leads to slower combustion due to lower oxygen concentration, $Y_{O_2,itk}$, and thus lower peak pressure and temperature. As widely reported, the most important factor for NO_X production is the local combustion temperature that can be reduced by the bulk gas temperature diminution [40]; thus the temperature change has a dramatic effect on NO_X emissions. On the other hand, when the EGR rate increases while maintaining the fuel mass m_f, the imep and bmep decreases due to the slower combustion. The bsfc shows the opposite trend

than the bmep.

		B10 [°]	B50 [°]	B90 [°]	p_{max} [bar]	T_{max} [°C]	imep [bar]	bmep [bar]	bsfc [g/kWh]	NO_X [ppm]	Soot [FSN]
EGR	0	2.7	9.4	25.6	106	1540	10.6	3.6	504	1101	0.13
[%]	30	3.9	10.6	34.6	98	1447	10.4	3.5	523	156	2
p_{itk}	1.4	3.6	10.4	33.4	92	1582	10.4	3.5	530	493	0.51
[bar]	1.8	2.6	9.6	26.4	113	1443	10.8	3.7	493	581	0.17
T_{itk}	41	3.6	10.2	29.2	103	1474	10.4	3.6	499	521	0.24
[bar]	61	3.6	10.4	29.8	102	1512	10.4	3.5	522	560	0.27
SOI_{pil}	-38	3.6	10.2	29.8	102	1480	10.4	3.5	516	530	0.24
[°]	-30	3.4	10.2	29.8	103	1489	10.4	3.5	519	544	0.24
SOI_{main}	-9	-1.1	5.6	23.0	117	1546	10.5	3.6	503	791	0.18
[°]	-1	7.3	14.2	35.0	87	1447	10.2	3.3	547	387	0.51
p_{inj}	1035	2.8	10.8	32.8	100	1483	10.4	3.9	476	474	0.51
[bar]	1435	2.3	8.6	25.6	107	1519	10.5	3.4	545	632	0.15

Table 3: Values of in-cylinder parameters and output parameters in the simple effect tests.

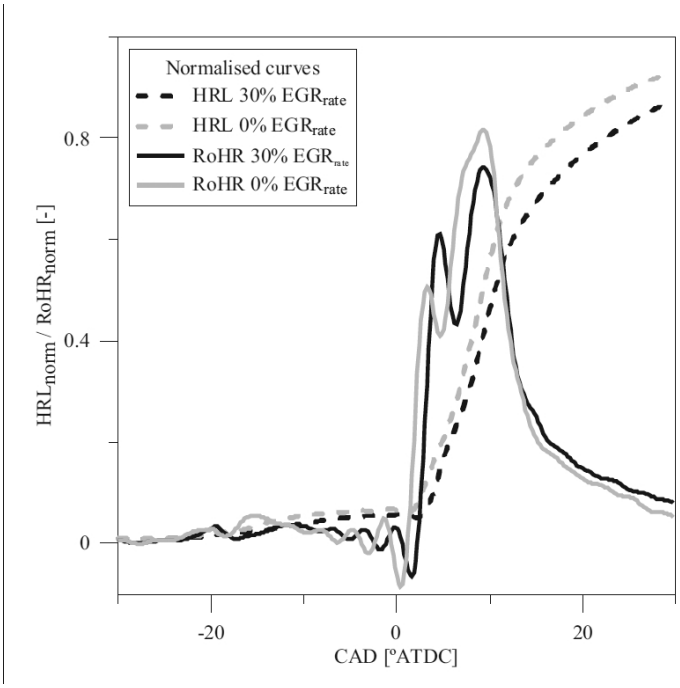

Figure 2: Comparison between rates of heat released at 0% and 30% of EGR.

The second parameter to analyse is the intake pressure p_{itk}. The pressure range was

set according to the 4-cylinder engine possibilities, while keeping the soot emissions lower to 2 FSN. Thus, it was increased from 1.4 to 1.8 bar in three levels (range centred on the reference value) at constant fuel mass and EGR rate, thus changing the air/fuel ratio. Increasing p_{itk}, and thus oxygen concentration, leads to higher combustion speed, peak pressure and peak temperature, and hence higher flame temperature that produces an increment of NO_X emissions. The effect on imep, bmep and bsfc has the opposite trend than EGR.

In the 4-cylinder engine version, the exhaust pressure is a consequence of p_{itk} and the turbocharger performance. Available results showed that a change of 100 mbar in p_{exh} leads to pmep variations of about 50 mbar, which affects less than 1% to bmep. This parameter was set 100 mbar above the intake pressure in all the operating points, as in the reference operating point.

Although the inlet temperature can be widely modified in a single-cylinder test bench, it was swept in a range of 20 ℃ (from 40 to 60 ℃), to be realistic with actual operating conditions in the 4-cylinder engine version. As T_{itk} increases while maintaining p_{itk}, lower density and trapped mass is obtained, and fuel air ratio increases. The lower spray mixture rate and oxygen concentration lead to a combustion slowdown. It has a minor effect on in-cylinder pressure and imep, and thus bmep and bsfc slightly worsen. The effect on in-cylinder pressure is not enough to compensate the higher gas temperatures produced by the T_{itk} increase; hence NO_X emissions increase. However, apart from the pilot injection setting, T_{itk} is the parameter with the smallest effect in comparison with the rest. Thus it was discarded for the detailed experimental DOE.

Once the intake conditions were analysed, the injection settings parameters were studied. The combustion process is very sensitive to the start of the main injection, SOI_{main}. The variation range of both the pilot and main injection were set to $\pm 4°$. As the reference settings are limited by the engine emissions, combustion is not optimally centred and thus, when SOI_{main} is advanced, the bsfc decreases due to the improvement of the indicated cycle. Peak pressure and gas temperature increase because combustion takes place earlier at the compression stroke; as expected [33], this leads to higher NO_X emissions due to the local flame temperature increase.

The start of the pilot injection, SOI_{pil}, (about 10% of the fuel mass) shows a minor effect on all the parameters. It was found that SOI_{pil} only affects significantly the rate of change of the pressure and thus noise, which is out of the scope of this work. However, it hardly modifies the heat release, performances and NO_X emissions. SOI_{pil} was discarded for the detailed study due to its low effect, in comparison with the rest of parameters, in particular with SOI_{main}.

The last parameter to consider is the injection pressure p_{inj}. Since it speeds up or slows down the combustion, it is one of the most influential parameters to consider. A variation range of ± 200 bar was set; it allows getting appreciable effect on the heat release (15% variation on maximum heat release) while having NO_X and performance variations similar to the rest of parameters (consumption changes less that the rest while NO_X variation is higher). When the injection pressure increases, both the peak pres-

sure and temperature increase and thus the NO_X emissions becomes higher. Due to the enhanced combustion velocity the imep increases because the combustion centring is improved. However, this is compensated because of the higher power demanded by the injection pump, which may lead to a lower bmep and higher bsfc.

This simple effect analysis is suitable for a straightforward comprehension of the effects on emissions and performance. However, engine behaviour is not lineal, and injection and air management strategies lead to complex interactions that are not easy to predict when several parameters change at the same time. Moreover, simple effect parametric studies usually do not allow reaching a global optimum. These problems were faced using the RSM, as described at the following sections.

5. Calculation of the in-cylinder parameters response surfaces

The first step in the model development is the calculation of the correlations between the in-cylinder parameters and the inputs. The burned angles (B%), the in-cylinder peak pressure and the imep were considered the combustion observers to evaluate. Its correlations are based on the statistic, however, the simple effect analysis allowed checking that RSM provides both reliable and physically coherent expressions.

5.1. Burned angles

The most important source of information regarding the combustion development is the heat release law. If in-cylinder pressure is available, B% expressions should not be necessary for the outputs prediction (because the real ones could be calculated); however, there are some reasons to model it. The first is that some burned angles such as B50 are typically used to control the combustion evolution [29] and thus, knowing the relationship between burned angles and inputs allows determining the required inputs to reach the desired B% during control operation or input parameter optimisation, as will be shown. The second is that the B% calculation is faster that accurate heat release calculation; thus, using the modelled B% is a good solution in case that the time limitation was critical (with a small penalty in the engine outputs prediction). The effect of considering the modelled or experimental B% on output predictions will be discussed later.

The RSM was applied to correlate the burned angles with the input parameters with a 5% step (B5, B10...B95), obtaining expressions such as Eq. (2) for the most relevant burned angles.

$$\begin{aligned}
B10 &= 22.4 - 26.7 \cdot Y_{O_2,itk} + 1.05 \cdot SOI_{main} - 2.30 \cdot p_{itk} - 0.001 \cdot p_{inj} - 0.2 \cdot m_f - 0.04 \cdot SOI_{pil} \\
B15 &= 21.34 - 19.3 \cdot Y_{O_2,itk} + 1.04 \cdot SOI_{main} - 2.20 \cdot p_{itk} - 0.003 \cdot p_{inj} \\
B25 &= 20.81 - 16.5 \cdot Y_{O_2,itk} + 1.03 \cdot SOI_{main} - 1.28 \cdot p_{itk} - 0.003 \cdot p_{inj} \\
B50 &= 28.5 - 25.5 \cdot Y_{O_2,itk} + 1.06 \cdot SOI_{main} - 1.31 \cdot p_{itk} - 0.005 \cdot p_{inj} \\
B75 &= 61.6 - 88.7 \cdot Y_{O_2,itk} + 1.44 \cdot SOI_{main} - 7.11 \cdot p_{itk} - 0.008 \cdot p_{inj} \\
B90 &= 113.1 - 173.9 \cdot Y_{O_2,itk} + 1.37 \cdot SOI_{main} - 12.30 \cdot p_{itk} - 0.017 \cdot p_{inj}
\end{aligned} \tag{1}$$

with a mean R^2=99.5%. Similar accuracy was found using EGR in expressions 2 instead of $Y_{O_2,itk}$; however, the oxygen concentration was preferred because it is the physical variable that is modified with the EGR and it is also used to model NO_X emissions in section 6.2.

The ANOVA analysis and Pareto's charts [34] in Fig. 3 show that, at the first combustion stages, m_f, T_{itk} and SOI_{pil} must be considered in order to get a good response. The effect of SOI_{pil} at the first part of the combustion can easily be justified, while T_{itk} has a direct effect on combustion delay. The effect of m_f at the first combustion stages (from SOC to B10) can be explained because one of the causes of the small fuel variation is the instability of the fuel injected in the pilot injection. When B15 is reached, the influence of such inputs decreases from 4%, 3.2% and 1.2% respectively, to less than 0.5%. They are negligible from B50 onwards (see Fig. 3). In all the cases EGR ($Y_{O_2,itk}$), SOI_{main}, p_{itk} and p_{inj} have a significant effect.

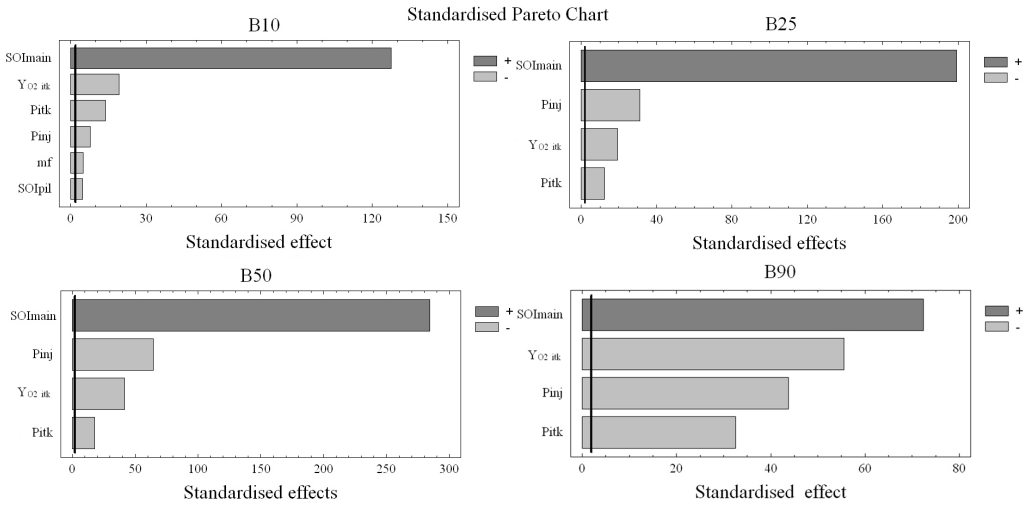

Figure 3: Pareto charts for B10, B25, B50 and B90.

Looking at the fitting constants in Eq. (2), it can be stated that the weight of each input follows almost a monotonous trend when the combustion angles are higher to B15. The global trends are coherent with the simple effect analysis performed: the higher the EGR rate and SOI_{main} are, and the lower p_{itk} and p_{inj} are, the combustion is more delayed and slowed down. This effect is enhanced as B% increases, because fitting constants become higher. Moreover, the monotonous trend obtained from B15 to B90 allowed to build a global burned angles model with a R^2=99.3%:

$$B\% = B_1 + B_2 \cdot Y_{O_2,itk} + B_3 \cdot SOI_{main} + B_4 \cdot p_{itk} + B_5 \cdot p_{inj} \tag{2}$$

where:
$B_1 = 2.6 \times 10^{-6} \cdot \%^4 - 2.32 \times 10^{-4} \cdot \%^3 + 4.18 \times 10^{-3} \cdot \%^2 + 0.33 \cdot \% + 8.95$
$B_2 = -7.38 \times 10^{-7} \cdot \%^4 - 4.00 \times 10^{-4} \cdot \%^3 + 3.43 \times 10^{-1} \cdot \%^2 - 9.12 \times 10^{-1} \cdot \% - 12.00$
$B_3 = 5.55 \times 10^{-8} \cdot \%^4 - 9.49 \times 10^{-6} \cdot \%^3 + 5.9 \times 10^{-4} \cdot \%^2 - 0.01 \cdot \% + 1.15$

$$B_4 = 1.11 \times 10^{-6} \cdot \%^4 - 2.65 \times 10^{-4} \cdot \%^3 + 0.01 \cdot \%^2 - 0.41 \cdot \% + 1.38$$
$$B_5 = 1.84 \times 10^{-9} \cdot \%^4 - 2.84 \times 10^{-7} \cdot \%^3 + 1.47 \times 10^{-5} \cdot \%^2 - 2.16 \times 10^{-4} \cdot \% + 2.75 \times 10^{-3}$$

being % the percentage of energy released (with respect to the total fuel energy)

As will be explained, the engine outputs are described in terms of burned angles from B15 to B90; thus, the first and last parts of the combustion, with a more complex or uncertain behaviour, are not necessary. In order to check the model performance, it was tested at different operating points, different from that used for the model fitting, inside the region of interest. As an example, Fig. 4 shows the predicted and real instantaneous heat release evolution from B15 to B90, in 3 operating points with different EGR rate, SOI_{main} and p_{inj}. The mean relative error between experimental and modelled HRL is hardly 2%.

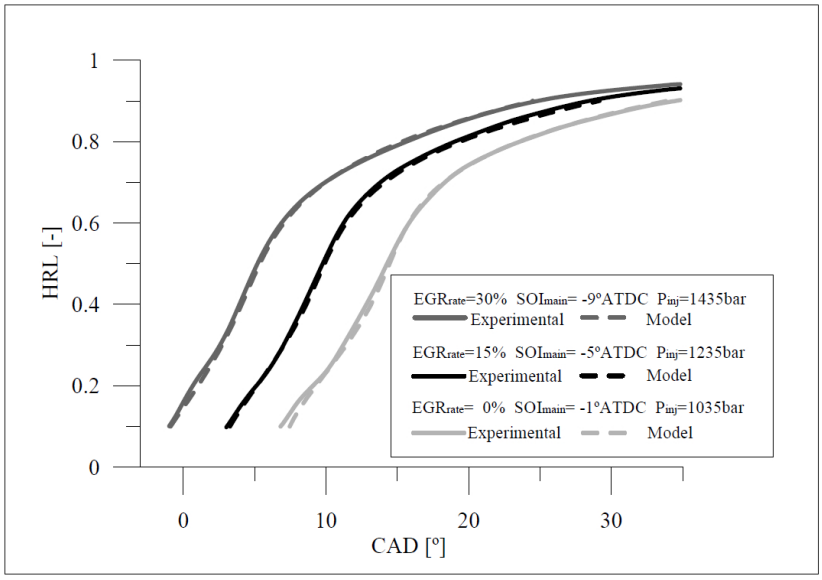

Figure 4: HRL experimental vs. modelled with RSM.

5.2. Maximum pressure p_{max}

The peak pressure is an input of the friction model proposed for the bmep prediction; additionally, it must be controlled during the engine operation in order to avoid reaching the mechanical limits. Thus, p_{max} was modelled and controlled during the input parameter optimisation.

As shown in Fig. 5a, the most influential input parameters are SOI_{main} and p_{itk}; this is coherent with the results obtained in the simple effect tests (see Table 3). The response surface obtained is:

$$p_{\max} = -102.06 + 175.91 \cdot Y_{O_2,itk} - 3.44 \cdot SOI_{main} + 46.11 \cdot p_{itk} + 0.018 \cdot p_{inj} + 2.72 \cdot m_f \quad (3)$$

with an R^2 of 99.3%.

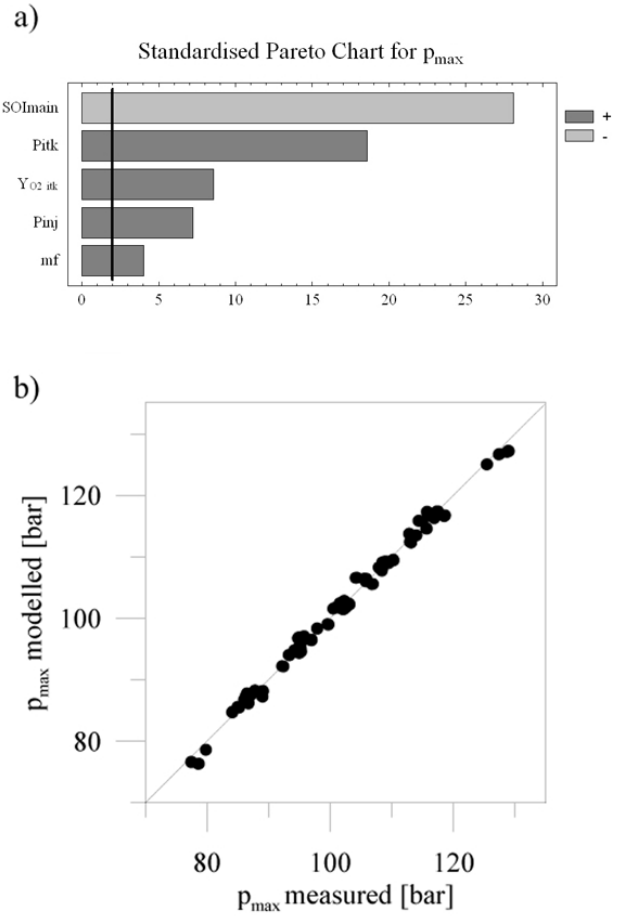

Figure 5: (a) Pareto chart for p_{max} prediction, (b) Scatter plots of p_{max} prediction.

5.3. Indicated mean effective pressure imep

The imep feeds the bmep and bsfc models as described in section 6. As in the case of burned angles, modelled imep provides a faster alternative to obtain the engine performance; avoiding the slower (although more accurate) calculation from in-cylinder pressure. The effect of considering the modelled or experimental imep on the output prediction will be discussed later.

The ANOVA analysis allowed discarding the less relevant inputs for the imep modelling, obtaining the following expression with an R^2=97.1%:

$$imep = -4.11 + 4.98 \cdot Y_{O_2,itk} - 0.045 \cdot SOI_{main} + 1.18 \cdot p_{itk} + 0.003 \cdot p_{inj} + 0.53 \cdot m_f \quad (4)$$

Analysing the results obtained throughout the Pareto's Chart (Fig. 6a), the most important inputs are the injected fuel mass m_f followed by the p_{itk}. The effect of m_f is obvious, while increasing p_{itk} leads to diminish fuel-air ratio thus enhancing a faster

combustion thanks to the higher O_2 concentration. The SOI_{main} has a deep impact on the combustion centring, and increasing the EGR rate leads to a slower combustion, as justified in section 4. Finally, the p_{inj} variation is the smallest statistically significant effect. Figs. 5b and 6b show the modelled and experimental p_{max} and imep obtained. Accordingly to the stated R^2 values, both of them show a good agreement, specially the p_{max}.

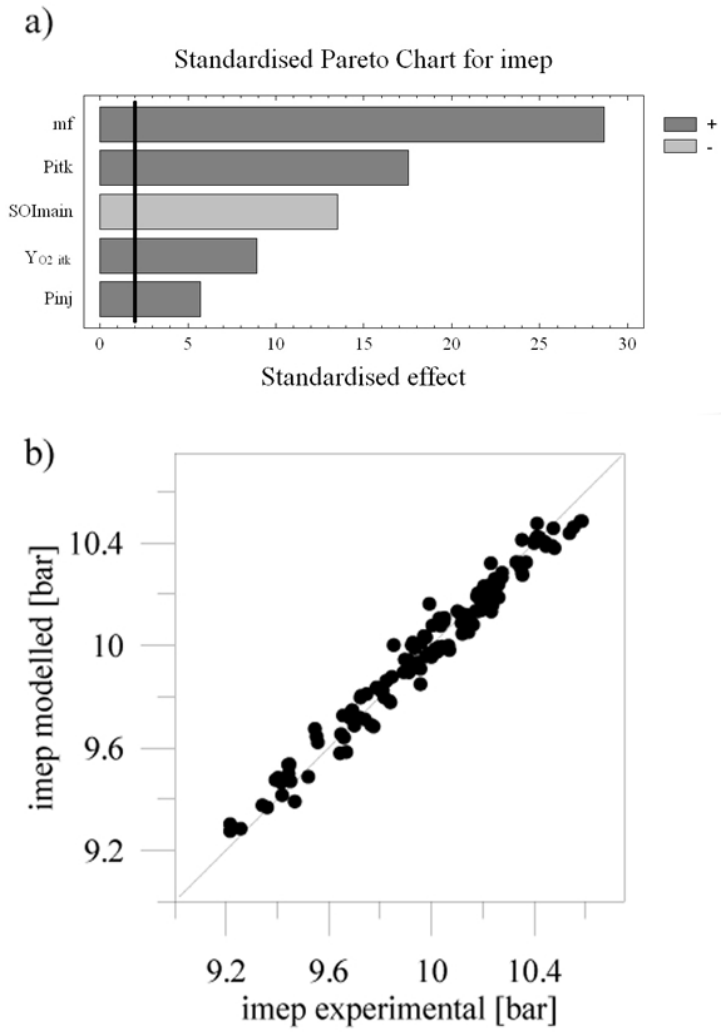

Figure 6: (a) Pareto chart for imep prediction, (b) Scatter plots of imep prediction.

6. Calculation of the outputs response surfaces

Starting from the measured or modelled in-cylinder parameters, the NO_X emissions and brake parameters were obtained. Engine performance is derived from imep using a

mechanical losses model, while the most relevant information for the prediction of NO_X emissions was assumed to be the heat release law [27].

6.1. Mechanical losses model

Mechanical losses are dissipated in three different paths [41, 42, 43, 44]. The most important is the friction due to the relative movement of some engine parts. The second term is the pumping work. However, as explained in section 2, the pressure difference between inlet and exhaust was kept constant in all the operating conditions, and thus pumping work does not change. In multi-cylinder engines, with variable inlet and exhaust conditions, the pumping work could be directly obtained from in-cylinder pressure or modelled, in terms of the most relevant engine inputs, as shown for other in-cylinder parameters. Finally, the last term is the energy required to move the auxiliary systems [41, 43, 44]. As the operating points were performed at constant engine speed, no significant variation of coolant and oil pumps power was expected; hence, they were externally operated. However, the power to move the fuel pump change a big amount when the rail pressure is modified.

The following section deals with the modelling of these terms.

6.1.1. Friction and auxiliaries mean effective pressures

The first friction term modelled is the injection pump work, which is easier to obtain than friction. The injection pump of a common rail system can be calculated according to:

$$N_f = \frac{Q_f \cdot \Delta p_f}{\eta_f} \tag{5}$$

where Q_f is the fuel volumetric flow, $\Delta p_f \approx p_{rail}$ is the pressure pump increase, and η_f is the pump efficiency.

The volumetric flow supplied by the pump, hardly changes with neither pressure nor fuel mass injected, being roughly proportional to the engine speed, according to $Q_f = k_{1_f} \cdot n$, where k_{1_f} is a fitting constant. Thus, the pumping work can be calculated as:

$$N_f = \frac{k_{1_f} \cdot n \cdot p_{rail}}{\eta_f} = k_f \cdot n \cdot p_{inj} \tag{6}$$

where $k_f = \frac{k_{1_f}}{\eta_f} = 1.42 \cdot 10^{-7}$ was fitted through the pump characterisation using some n and p_{inj} swepts in whole engine map.

Finally, the auxiliary mean effective pressure, amep, is calculated in the following way:

$$amep = \frac{N_f}{0.5 \cdot n \cdot V_t} = \frac{k_f \cdot p_{inj}}{0.5 \cdot V_t} \tag{7}$$

where V_t is the displaced volume.

Once the amep is known, the friction mean effective pressure can be obtained from the difference between net imep minus amep, and bmep. Following to Heywood [41] and

Macek [44] the fmep can be correlated with the engine load and speed. Eq. (8) was used to model it; the effect of engine load is considered through p_{max}, the linear piston speed c_m allows considering the effect of the engine speed and k_1, k_2 and k_3 are fitting constants.

$$fmep = k_1 + k_2 \cdot p_{\max} + k_3 \cdot {c_m}^2 \tag{8}$$

Taking into account that the tests were performed at constant engine speed, $k_1 + k_3 \cdot {c_m}^2$ can be grouped into a single constant K_p, obtaining:

$$fmep = K_p + k_2 \cdot p_{\max} \tag{9}$$

where $K_p = 448600$ and $k_2 = 4.5 \cdot 10^{-3}$ with p_{max} and fmep in [Pa].

6.1.2. Brake specific fuel consumption

Once the friction terms were calculated, the brake mean effective pressure was obtained as:

$$bmep = imep - fmep - pmep - amep \tag{10}$$

where fmep is obtained with Eq. (9) and amep with Eq. (7). If the experimental in-cylinder pressure is available, imep, pmep and $p_{\max}$ can be calculated directly from it. If the in-cylinder pressure is not measured, the modelled imep and $p_{\max}$ (see Eq. (4) and (3)) can also be used. In both the cases, the brake specific fuel consumption can be directly derived:

$$bsfc = \frac{m_f}{bmep \cdot V_t \cdot n \cdot 0.5} \tag{11}$$

Using modelled imep and $p_{\max}$ the bsfc model shows a slightly poorer fitting (R^2 = 92.2%) than using experimental data from measured in-cylinder pressure, as shown in Fig. 7. The R^2 increases in the last case up to 96.7%, being the mean error between measurements and predictions about 2%. This is a good result that allows highlighting the interest of using experimental p_{cyl}, if it is available.

6.2. NO_X emission model

According to different authors [19, 27, 45], Diesel engines NO_X emissions is mainly produced following thermal and prompt mechanisms. According to Benajes et al. [33] the prompt mechanism is strongly related to low temperatures reactions and it contributes a small fraction to the total NO_X quantity, while thermal NO_X is the most important factor and it depends on the reaction temperature and the local air fuel ratio.

As assumed in a previous work [27], fuel burns stoichiometrically in a region where the fuel/air equivalence ratio is close to 1 and the gas temperature is close to the adiabatic temperature. Hence, the instantaneous NO_X production can be correlated with the rate of heat release, and thus burned angles were selected as key parameters to predict NO_X emissions. To take into account the effect of the fuel/air equivalence ratio on NO_X emissions, both the intake oxygen mass fraction, $Y_{O_2,itk}$ and fuel mass were also included

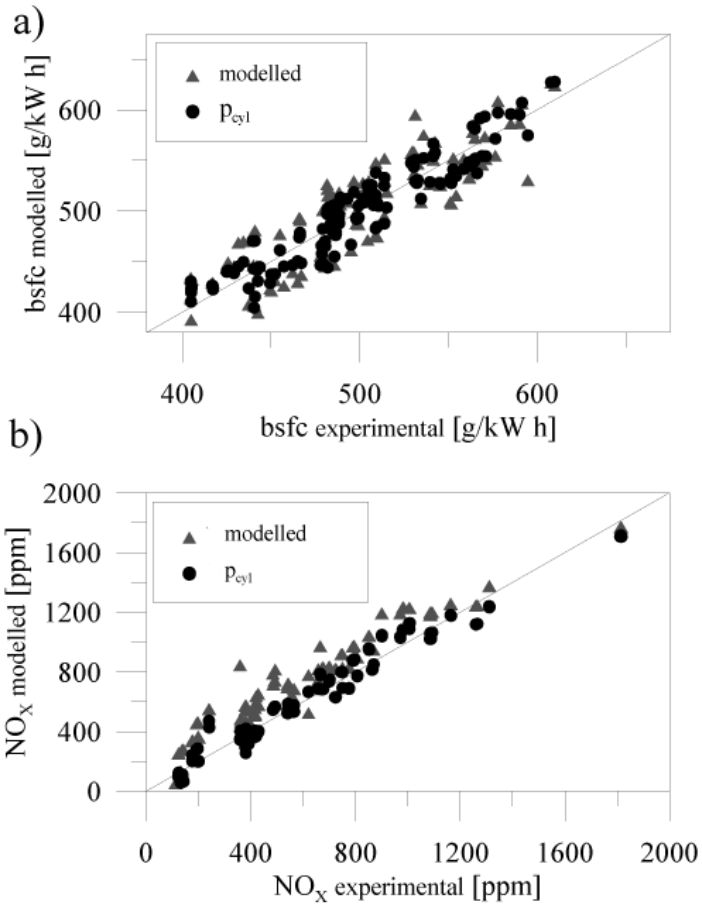

Figure 7: (a) Pareto chart for NO_X prediction, (b) Response surface for modelled NO_X.

in the NO_X modelling. Applying the RSM, the expression obtained to estimate the NO_X emission was:

$$\begin{aligned} NO_X = 8729.17 - 44.32 \cdot B15 - 58.37 \cdot B50 - 28.08 \cdot B70 \\ +60.86 \cdot m_f - 99790.5 \cdot Y_{O_2,itk} + 280943 \cdot Y_{O_2,itk}^2 \end{aligned} \quad (12)$$

with a R^2=96.5%.

According to the results obtained in the ANOVA analysis shown at Fig. 8, the most influencing parameter is the O_2 concentration at the inlet. This result is in good agreement with the EGR effect obtained in the simple effect study. It is also interesting to highlight that $Y_{O_2,itk}$ has a direct effect on the combustion velocity, which is taken into account throughout the B% variation in Eq. (12) (see EGR effect on Table 3). However, there is an additional effect that is considered with the $Y_{O_2,itk}$ terms in Eq. (12). That

is, if the combustion took place with the same rate of heat release but different oxygen concentration in the chamber, the adiabatic temperature would be different and also the NO_X production. This effect justifies the necessity to include $Y_{O_2,itk}$ terms in the NO_X correlation to reach good accuracy.

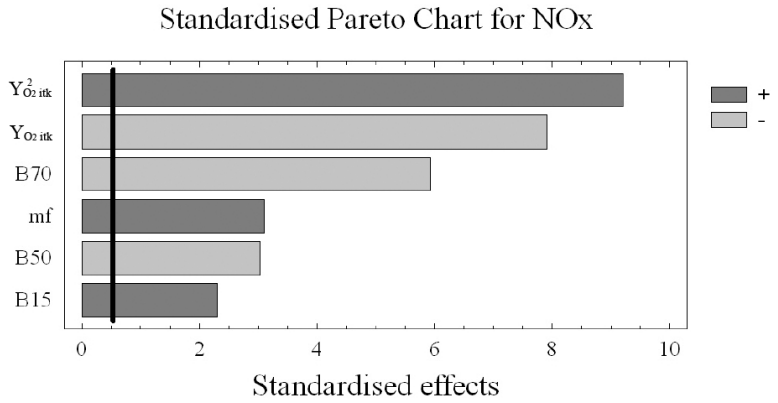

Figure 8: Comparison between predictions of bsfc and NO_X, with in-cylinder pressure data vs. input parameters data.

The burned angles B15, B50 and B70 provide a complete tracking of the combustion development. It was checked that some other combinations (for example including B25 and B90) can also be valid, but this was the simplest option with a high correlation. It was also checked that removing the initial or final combustion information (B15 and B70) lead to reduce the R^2 drastically. When burned angles change, the global trend of NO_X in Eq. (12) is in agreement with the effect of the combustion phasing obtained in the simple effect analysis. Hence, as can be seen in Table 3, delaying or slowing down the combustion (by changing EGR, p_{itk}, SOI_{main} or p_{inj}) leads to diminish the NO_X emissions.

Finally, the fuel mass is also included in the Eq. (12) since the NO_X produced is sensitive to any change in this parameter as derived from Fig. 8. This can be justified easily taking into account that a variation of 5% of the total fuel mass injected affects almost proportionally to the amount of NO_X produced.

If the modelled B% obtained with Eq. (2) were used in Eq. (12) instead of the experimental ones, the model accuracy is a bit lower, and R^2 decreases to 95.5%. However, even this accuracy is quite good, and additionally the calculation time is 1.5 ms vs 5.5 ms in the case of calculating the experimental heat release from in-cylinder pressure using a simplified in-house combustion diagnosis tool [27]. This is a good reason to consider both the paths: the faster, using inputs parameters, or the more accurate, from experimental in-cylinder pressure. Fig. 7 shows a scatter plot of predicted vs experimental NO_X using experimental and modelled B%, in all the operating conditions. The global mean errors are about 6% and 14%, using experimental or modelled B% respectively. This results

are better than other models with similar features found in literature [17, 18, 30].

7. Output parameters optimisation

The simplest way to optimise factors is varying them in a wide range and different levels simultaneously [30, 35]. Nevertheless, it is an expensive approach due to the experimental work required. To limit the experimental measurements, the COST method (Changing One Separate factor at a Time) is classically used; however, the main drawback of this method is that it can not find the optimum if there are interactions between factors [34]. If this technique is combined with the "try and error" method [4, 29], good results can be found; hence, some authors [5, 46] claim to have obtained satisfying results in Diesel engines using this combination. However, the optimisation methods based on models is an efficient option to avoid increasing the experimental work unnecessarily. As an example of the possibilities offered by the proposed model, Fig. 9 shows some NO_X-bsfc modelled maps, obtained with different inputs combinations. In all cases, the central point corresponds to the reference conditions. On one hand, the trends obtained in the simple effect analysis are well identified at this figure. Thus, subplots a), b) and d) show that increasing EGR rate, maintaining the rest of parameters, leads to lower NO_X and higher consumption. An earlier SOI_{main} improves consumption but increases NO_X emissions dramatically, as shown at subplots a), c) and e). Increasing inlet pressure produces a lower bsfc but higher NO_X emissions, as seen at subplots b), c) and f). Finally, decreasing the rail pressure improves both the consumption and NO_X emissions (see subplot d), e) and f)).

On the other hand, looking at the slope of the iso-parameter curves, the best option to optimise NO_X or consumption can be identified. Thus, EGR (see a), b) and d)) and SOI (in c) and e)) are the best parameters to modify NO_X, because their curves are much more perpendicular to the NO_X axis than the other parameters, and thus the input modification affects importantly the NO_X and slightly the bfsc. In the case of bsfc, the rail pressure seems to be the most promising option (see d) and e)), while input pressure affects to both the emissions and consumption.

When both the consumption and NO_X emissions have to be improved, depending on the priority, different combinations of two input parameters allow moving the operating point towards the best direction in Fig. 9. Individual target optimisation are easy to be conducted, but the combination of two or more targets makes the process difficult. If some restrictions have to be imposed additionally [33], the optimization becomes almost impossible. In this case, working with modelled maps such that plotted in Fig. 9 is not the best option, and the multi-objective optimisation has to be applied, allowing automating the process of finding the optimum.

When the optimization deals with several inputs and outputs, the way to set the best direction is defining a cost function that weights some response parameters into a single merit value [2, 31, 33, 34, 47]. Depending on the outputs priority, different inputs combinations would be reached. Following a previous work developed at the authors' research group [33], the merit function proposed is:

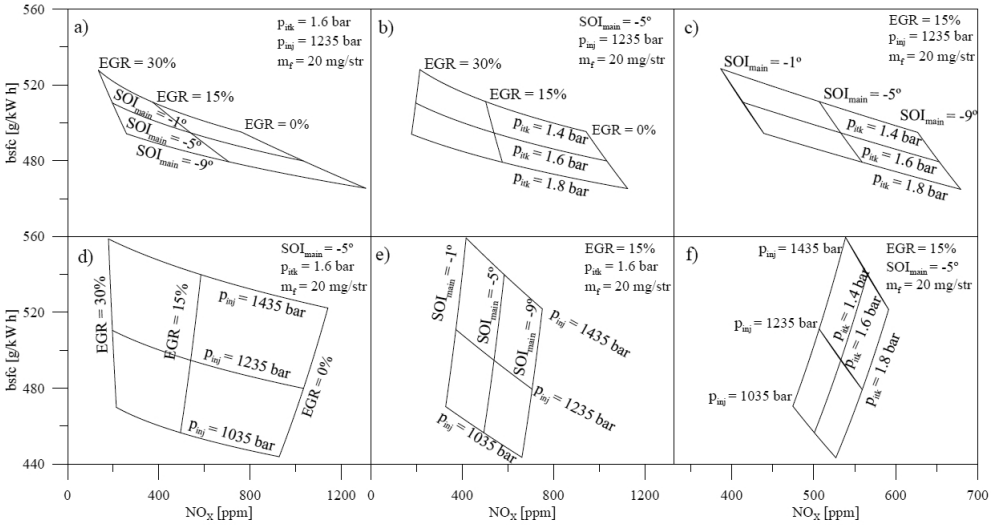

Figure 9: Relation between input parameters vs. bsfc and NO_x modelled: (a) EGR and SOI_{main} swept at nominal P_{itk} and P_{inj}, (b) EGR and P_{itk} swept at nominal SOI_{main} and P_{inj}, (c) P_{itk} and SOI_{main} swept at nominal EGR and P_{inj}, (d) EGR and P_{inj} swept at nominal SOI_{main} and P_{itk}, (e) P_{inj} and SOI_{main} swept at nominal EGR and P_{itk}, (f) P_{itk} and P_{inj} swept at nominal EGR and SOI_{main}.

$$Merit = \frac{1000 \cdot \sum_i (\alpha_i)}{\sum_i \left(\alpha_i \cdot e^{\beta_i \cdot \frac{(Output_i - Target_i)}{Target_i}} \right)} \tag{13}$$

where $Output_i$ is the response variable i (NO_X and bfsc), $Target_i$ is the target of the response variable i, α_i is the weight factor of the response variable i and β_i is the gradient of the merit near the optimum. Fig. 10 shows the effect of α and β. On one hand, the value of α in Fig. 10a allows to set the priority of the output during the optimisation. On the other hand, the effect of β_i on the merit is shown in Fig. 10b. Its value allows selecting the importance of being very close to the target and thus, it affects the flexibility for finding different alternatives solutions. It is important to realise that α_i can be selected with no limit, depending on the preferred output; however β_i can not be chosen arbitrarily because the optimisation process could not converge to a good solution or not converge at all. For example, in the case of NO_X shown in Fig. 10b, the β have to be about 1 or lower to ensure that a small decrease of the NO_X emissions (with respect to the base-line) increases the merit value. If not, the NO_X would not be properly considered because, starting from the base-line, there is no clear merit improvement when NO_X diminishes in a small amount.

Using the described NO_X and consumption models to feed the optimiser, the optimisation was carried out starting from the reference operating point defined by the ECU setting (base-line). The objective is finding an inputs combination with lower NO_X and bsfc. The multi-objective optimisation is flexible to include different restrictions such as

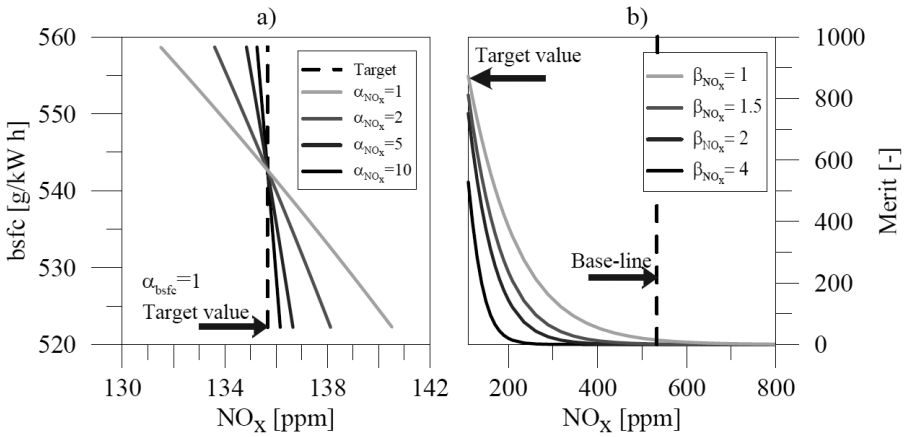

Figure 10: (a) Effect of weight α on the relationship between NO_X and bsfc. (b) Sensitivity study of β to evaluate the effect on merit value.

limiting p_{max}, maintaining torque or combustion angles, etc. It was imposed to maintain the fuel mass injected, to limit the peak pressure to the nominal value, 102 bar (thus ensuring that mechanical load does not worsen), and to vary the combustion centring (B50) less that 3°. The range of the inputs was limited to the boundaries stated in Table 2, were the model accuracy has been validated.

Three different strategies were used for the optimisation: the first gives priority to the NO_X reduction (α_{NO_X}=100, α_{bsfc}=1), the second assumes the same importance for NO_X and consumption, and the third gives more importance to the consumption (α_{NO_X}=1, α_{bsfc}=100). In all the cases, the NO_X and consumption targets were set to NO_X = 100 ppm and bsfc = 450 g/kW h. Table 4 shows the nominal and the optimised results. It is interesting to highlight that bsfc target was set to such high value because in single-cylinder engines the mechanical losses have a great effect on consumption.

As can be seen, NO_X improves in all the cases, mainly due to the EGR level, which is optimised to the maximum admitted value in the three optimisations, independently of the priority given to NO_X and bsfc. The reason is that EGR has a dramatic effect on NO_X while it has a moderate effect on consumption (see Table 3); thus, the optimal value increases because the NO_X improvement effect on the merit is higher that the consumption worsening. Hence, the consumption only improved in the two cases where it had similar or higher weight that NO_X.

Comparing the three optimisations it can be seen that when $\alpha_{NO_X} > \alpha_{bsfc}$ the SOI_{main} is delayed with respect to the nominal value, thus decreasing the mean temperature and helping to reduce NO_X emissions. Increasing injection pressure helps to keep the B50 centred. As a consequence of the contrary effects of EGR and SOI_{main}, and p_{inj} the peak pressure decreases slightly. Consumption increases because it was not a key issue during the optimisation.

Parameter	Unit	Nominal	α_{NO_X}¿α_{bsfc}	α_{NO_X}=α_{bsfc}	α_{NO_X}¡α_{bsfc}
		Weight			
α_{NO_X}	[-]	-	100	1	1
α_{bsfc}	[-]	-	1	1	100
		Inputs			
EGR	[%]	15	30	30	30
SOI_{main}	[°ATDC]	-5	-3	-3.6	-4.8
p_{itk}	[bar]	1.6	1.8	1.8	1.8
p_{inj}	[bar]	1235	1292	1060	1035
		Outputs			
NO_X	[ppm]	538	100	120	180
bsfc	[g/kWh]	491	525	472	465
B50	[°ATDC]	10.2	12.6	12.1	11.8
p_{max}	[bar]	102	100	101	102
bmep	[bar]	3.5	3.3	3.7	3.8
merit	[-]		861	959	1021

Table 4: Relative weights, inputs and outputs values using optimisation algorithms.

When the bsfc and NO_X importance is similar, the SOI_{main} is advanced to increase imep, and p_{inj} decreases to limit the auxiliary power; hence, bmep increases and bsfc is improved while controlling B50 variation. In this case, the NO_X shows a penalty of about 20 ppm and p_{max} increases about 1 bar with respect to the previous optimisation.

Finally, if the priority is to reduce the consumption, the SOI_{main} is advanced more and p_{inj} diminishes more, thus improving the indicated cycle and the bmep. In this case, the p_{max} reaches the maximum allowed value and NO_X shows an important penalty of about 80 ppm.

As shown, the proposed NO_X and bsfc predictive models are suitable to be used for optimisation applications that allows, depending on the objective, to set the best inputs to minimise NO_X, consumption or both of them. Although it is out of the scope of the paper, it must be highlighted that no soot information has been considered; thus, the optimisation results are not definite. However, the proposed models are flexible to include other emissions and restrictions.

8. Conclusions

This paper describes the development of a predictive model oriented to control and optimisation applications in DI Diesel engines. Taking into account that in-cylinder conditions provide a valuable information to predict engine performance and emissions, a methodology to develop a NO_X and bsfc models, based on in-cylinder parameters, have been presented.

The models are split in two parts: the first provides the in-cylinder parameters as a function of some engine inputs related to intake charge conditions (EGR, intake pressure) and injection settings (fuel mass, injection pressure, SOI_{main}); the second allows predicting NO_X and bsfc in terms of the in-cylinder parameters and a limited number of inputs. In both cases, the Response Surface Methodology was used to fit empirical expressions of burned angles, p_{max}, imep and finally NO_X. In all cases, it was checked that the correlations obtained are able to describe the physical trends analysed in a single effect study.

Regarding the in-cylinder parameters modelling, it was obtained a R^2 of 99.4% and 97.0% in the case of the p_{max} and imep respectively. It has also been proposed a global model to predict the heat release between B10 and B90 with a $R^2 = 99.4\%$, that allows to predict the combustion evolution in all the operating range tested. The good accuracy of the models has allowed using them as an input of the NO_X and bsfc models, instead of the experimental values obtained from in-cylinder pressure.

Starting from the experimental or modelled imep, the bsfc has been obtained by means of a simple mechanical losses model. Finally, the NO_X emissions has been estimated in terms of a limited number of burned angles, the fuel mass injected and the oxygen concentration at the inlet. It has been checked that modelled in-cylinder parameters allows predicting the engine response faster than using experimental data, while maintaining the good accuracy in case of NO_X emissions ($R^2 = 95.5\%$); although in case of imep the result was not so good ($R^2 = 92.5\%$). However, if the maximum precision was needed, using the experimental in-cylinder parameters improves the model accuracy more that 4% in the case of imep and 1% in the case of NO_X emissions. This result justifies the interest of using a split model to consider two paths: the faster, using input parameters, or the more accurate, from experimental in-cylinder pressure.

Using the predictive model to provide accurate values of NO_X and bsfc, a multi-objective optimisation process has shown the model potential and flexibility. Hence, using a merit function to set the optimization priority, it has been shown that different optimal inputs combinations are obtained, depending on the objectives. The method is flexible to include different restrictions related to in-cylinder parameters.

One of the most outstanding feature of the methodology and the model described is that they allowed considering a complete list of inputs related with the injection settings, air management and combustion parameters, contrary to the proposals of other authors that usually are focused on the disturbance of a very limited number of parameters. At the same time, the simplicity and the short calculation time has been maintained. The proposed models were fitted for a specific single-cylinder engine, and thus they can not be easily extrapolated to different engines; however, the methodology followed is general and it can be applied systematically to cover the complete engine map of a multi-cylinder DI Diesel engine.

Ackowledgments
The support of the Universitat Politcnica de Valncia (PAID-06-09) and Generalitat Valenciana (GV/2010/045) is greatly acknowledged.

References

[1] Dimopoulos P, Schni A, Eggimann A, Sparti C. Statistical methods for solving the fuel consumption/emission conflict on DI-Diesel engines. SAE paper 1999-01-1077; 1999.

[2] Montgomery DT, Reitz RD. Effects of multiple injections and flexible control of boost and EGR on emissions and fuel consumption of a heavy-duty Diesel engine. SAE paper 2001-01-0195; 2001.

[3] Stobart RK ,Challen BJ, Bowyer R. Electronic controls - Breeding new engines. SAE paper 2001-01-0255; 2001.

[4] Atkinson C, Mott C. Dynamic model-based calibration optimization: An introduction and aplication to Diesel engines. SAE paper 2005-01-0026; 2005.

[5] Bohn C, Stber P, Magnor O. An Optimization-Based Approach for the Calibration of Lookup Tables in Electronic Engine Control. Proceedings of the 2006 IEEE, Conference on Computer Aided Control Systems Design, Munich, Germany, 2006.

[6] Schiefer D, Maennel R, Nardoni W. Advantages of Diesel engine control using in-cylinder pressure information for closed loop control. SAE paper 2003-01-0364 ; 2003.

[7] Mayne DQ, Rawlings JB, Rao CV. Scokaert P.O.M. Constrained model predictive control: Stability and optimality. Automatica 2000;36:789-814.

[8] Garcia C, Morari P. Model predictive control: theory and practice. Automatica 1989;25:335-48.

[9] Findeisen R, Algwer F. An introduction to nonlinear model predictive control. 21st Benelux meeting on systems and control, Veldhoven, Holland, 2002.

[10] Tunestal P, Lewander M. Model predictive control of partially premixed combustion. First Workshop on Automotive Model predictive Control: Models, Methods and Applications, Lund, Austria, 2009.

[11] Kalogirou Soteris A. Artificial itelligence for the modelling and control of combustion process: a review. Prog Energ Combust 2003; 29:515-66.

[12] Sellnau MC, Matekunas F, Battiston P, Chang C, Lancaster D. Cylinder-pressure-based engine control using pressure-ratio-management and low-cost non-intrusive cylinder pressure sensors. SAE paper 2000-01-0932; 2000.

[13] Arcaklioglu E, Celykten I. A Diesel engine's performance an exhaust emissions. Appl Energ 2005;80:11-22.

[14] Celik V, Arcaklioglu E. Performance maps of a Diesel engine. Appl Energ 2005;81:247-59.

[15] Saerens B, Vandersteen J, Persoons T, Swevers J, Diehl M, Van den Bulck E. Minimization of the fuel consumption of a gasoline engine using dynamic optimization. Appl Energ 2009;86:1582-88.

[16] Togun NK, Baysec S. Prediction of torque and specific fuel consumption of a gasoline engine by using artificial neural networks. Appl Energ 2010;87:349-55.

[17] Egnell R., Combustion Diagnostics by Means of Multi-zone Heat Release Analysis and NO Calculation. SAE Paper 981424; 1998.

[18] Andersson M, Johansson B, Hultqvist A, Noehre C. A Predictive Real Time NO_x Model for Conventional and Partially Premixed Diesel Combustion. SAE Paper 2006-01-3329; 2006.

[19] Arregle J, López JJ, Guardiola C, Monin C. Sensitivity Study of a NO_X Estimation Model for On-Board Applications. SAE Paper 2008-01-0640; 2008.

[20] G.G. Zhu, C.F. Daniels and J. Winkelman, MEBT timing detection and its closed-loop control using in-cylinder pressure signal, SAE paper 2003-01-3266 (2003).

[21] Leonhardt S, Meller N, Isermann R. Methods for engine supervision and control based on cylinder pressure information. IEEE/ASME Trans. Mechatronics 1999;4:235-45.

[22] Desantes JM, Galindo J, Guardiola C, Dolz V. Air mass flow estimation in turbocharged Diesel engines from in-cylinder pressure measurement, Exp. Therm. Fluid Sci. (2010;34:37-47.

[23] Luján JM, Bermúdez V, Guardiola C, Abbad A. A methodology for combustion detection in Diesel engine through in-cylinder pressure derivative signal. Mech Syst Signal Pr 2010; 24: 2261-75.

[24] Hasegawa M, Shimasaki Y, Yamaguchi S, Kobayashi M, Sakamoto M, Kitayama N, Kanda T. Study on ignition timing control for Diesel engines using in-cylinder pressure sensor. SAE paper 2006-01-0180; 2006.

[25] Shimasaki Y, Kobayashi M, Sakamoto H, Ueno M, Hasegawa M, Yamaguchi S, Suzuki T. Study on engine management system using chamber pressure sensor integrated with spark plug. SAE Paper 2004-01-0519; 2004.

[26] Payri F, Broatch A, Tormos B, Marant V. New methodology for in-cylinder pressure analysis in direct injection Diesel engines - application to combustion noise. Meas Sci Technol 2005;16:540-47.

[27] Guardiola C, López JJ, Martín J, García-Sarmiento D. Semiempirical in-cylinder pressure based model for NO_X prediction oriented to control applications. Appl Therm Eng 2011;31:3275-86.

[28] Reitz R , Von der Ehe J. Use of in-cylinder pressure measurement and the response surface method

for combustion feedback control in a Diesel engine. Proc. IMechE Part D: J. Automobile Engineering 2006;220:1657-66.
[29] Beasley MG, Cornwell RCE, Egginton MA, Fussey PM, King R, Noble D, Salamon T, Truscott AJ, Landsmann G. Coordinated cylinder pressure based control for reducing Diesel emission dispersion. Advanced Microsystems for Automotive Applications 2006 VDI-Buch 2006;3:223-38.
[30] Win Z, Gakkhar RP, Jain SC, Battacharya M. Parameter optimization of a Diesel engine to reduce noise, fuel consumption and exhaust emission using response surface methodology. Proc. IMechE 219 Part D: J. Automobile Engineering 2005;219:1181-92.
[31] Desantes JM, López JJ, García JM, Hernández L. Application of neural networks for prediction and optimization of exhaust emissions in a H.D. Diesel engine". SAE paper 2002-01-1144; 2002.
[32] Tichý J, Gautschi G. Piezo-Elektrische Meβtechnik. Berlin: Springer; 1980.
[33] Benajes J, Molina S, DeRudder K, Amorim R. Optimization towards low-temperature combustion in a HSDI Diesel engine, using consecutive screenings. SAE Paper 2007-01-0911; 2007.
[34] Montgomery DC. Response surface methodology: process and product optimization using designed experiments. Chichester,UK: Wiley; 2004.
[35] Hernández JJ, Sanz-Argent J, Carot JM, Jabaloyes JM. Modelling of the auto-ignition angle in Diesel HCCI engines through D-optimal design, Fuel 2010;89:2561-68.
[36] Canova M, Garcia R, Midlam-Mohler S, Guezennec Y, Rizzoni G. A control-oriented model of combustion process in a HCCI Diesel engine. American control conference, USA , 2005.
[37] Payri F, Molina S, Martín J, Armas O. Influence of measurement errors and estimated parameters on combustion diagnosis. Appl Therm Eng 2006;26:226-36.
[38] Serrano JR, Arnau FJ, Dolz V, Piqueras P. Methodology for characterisation and simulation of turbocharged Diesel engines combustion during transient operation. Part 1: Data acquisition and post-processing. Appl Therm Eng 2009;29:142-49.
[39] Serrano JR, Arnau FJ, Dolz V, Piqueras P. Methodology for characterisation and simulation of turbocharged Diesel engines combustion during transient operation. Part 2: Phenomenological combustion simulation. Appl Therm Eng 2009;29:150-58.
[40] Ladommatos N, Abdelhalim S, Zhao H. Control of oxides of nitrogen from Diesel engines using diluents while minimising the impact on particulate pollutants. Appl Therm Eng 1998;18:963-80.
[41] Heywood JB. Internal Combustion Engine Fundamentals. New York, USA: McGraw-Hill; 1988.
[42] Sethu C, Leustek ME, Bohac SV, Filipi ZS, Assanis DN. An Investigation in Measuring Crank Angle Resolved In-Cylinder Engine Friction Using Instantaneous IMEP Method. SAE paper 2007-01-3989; 2007.
[43] Sandoval D, Heywood JB. An Improved Friction Model for Spark-Ignition Engines. SAE paper 2003-01-0725; 2003.
[44] Macek J, Fuente D , Emrich M. A Simple Physical Model of ICE Mechanical Losses. SAE paper 2011-01-0610; 2011.
[45] Aithal SM. Modelling of NO_x formation in Diesel engine using finite-rate chemical kinetics. Appl Energ 2010;87:2256-65.
[46] Edwards IM, Jutan A. Optimization and control using response surface methods. Computers Chem Eng 1997;21:441-53.
[47] Mallamo F, Badami M, Millo. Application of the design of experiments and objective functions for the optimization of multiple injection strategies for low emissions in CR Diesel engines. SAE paper 2004-01-0123; 2004.